Effects of 3D Magnetic Field Structure to MHD Equilibrium and Stability

- 3D MHD Equilibrium in Stellarator

Yasuhiro Suzuki

for the LHD experiment group

National Institute for Fusion Science
The Graduate University for Advanced Studies SOKENDAI
Toki, Japan
suzuki.yasuhiro@LHD.nifs.ac.jp

NINS
National Institutes of Natural Sciences

531st Wilhelm and Else Heraeus Seminar
Bad Honnef 30 April - 2 May, 2013

outline

1. Stellarator and Heliotron
2. 3D MHD equilibrium
3. 3D MHD equilibrium studies in LHD
    1. Beta limit
    2. Experimental study of 3D MHD equilibrium in LHD
    3. Identification of 3D plasma boundary by CCS method
4. Conclusion

What are stellarator and heliotron configurations?

Mercier classifies the magnetic configuration from the viewpoint of creating rotational transform.

C.Mercier, “Lectures in Plasma Physics”

- Toroidal current along the axis
- Torsion of the axis
- Modulation of flux surfaces

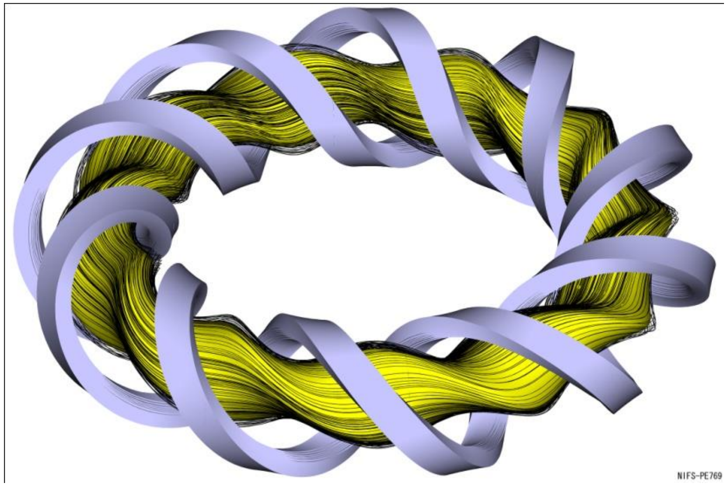

Stellarators create the rotational transform by 3D shaping.

Stellarator and heliotron have vacuum flux surfaces.
But, Tokamak and RFP make flux surfaces by the plasma itself. => strongly self-organized.

Stellarator is not disruptive

Collapsed events are observed but not disruptive!

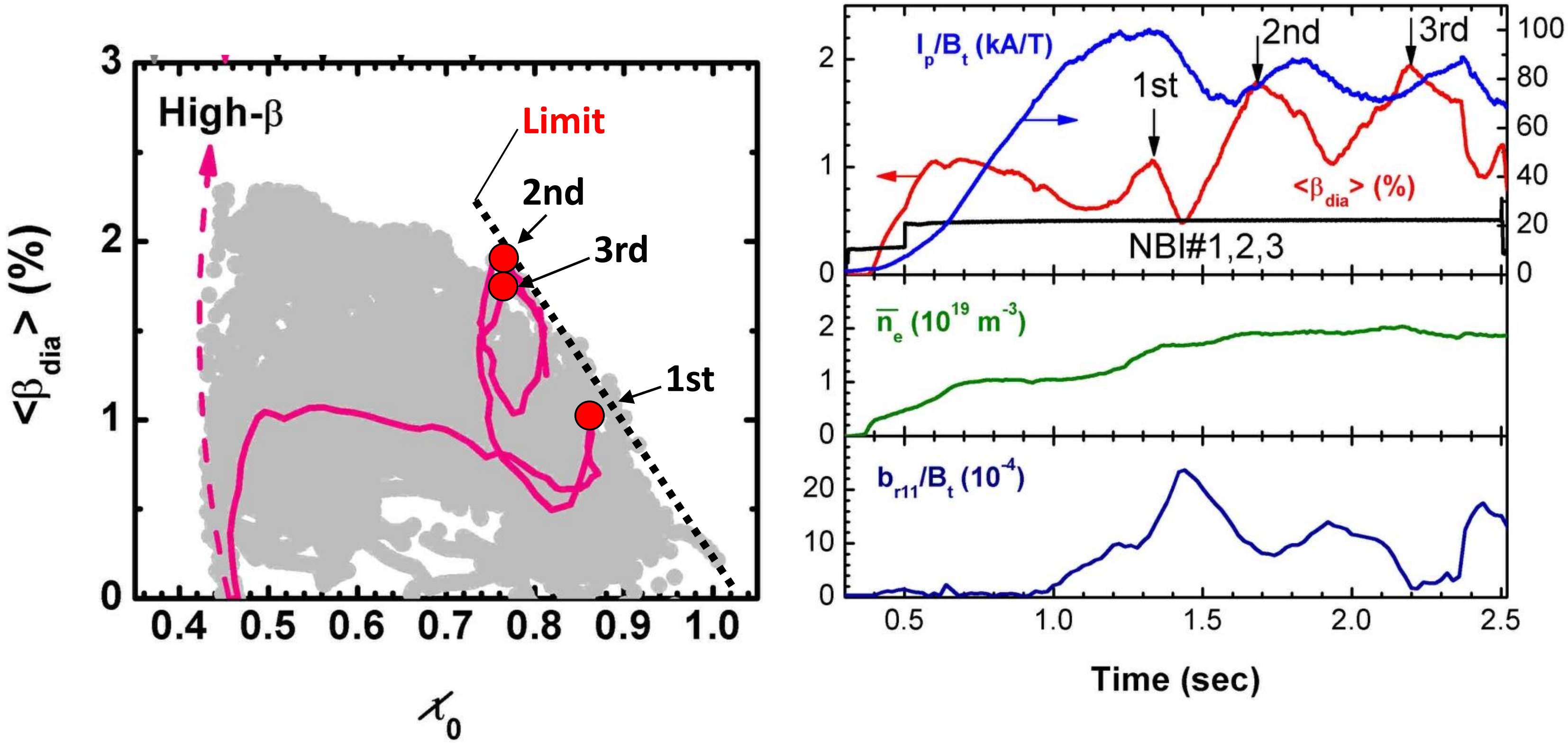

The total energy is minimum at the vacuum.

Classification of non-axisymmetric configuration

Stellarator and Heliotron configurations are intrinsically 3D!

3D nature in Tokamak and RFP

B_NA: non-axisymmetric field
B_A: axisymmetric field

Symmetry breaking by strong NA component : B_NA/B_A~1	**Stellarator-tokamak hybrid Helical axis core in tokamaks QSH in RFP**
Symmetry braking by weak NA components: B_NA/B_A~10^-3	Stabilization of RWM by RMP Error field mode ELM mitigation/suppression by RMP
Symmetry breaking by very week NA components: B_NA/B_A~10^-6~10^-5	TF ripple in tokamaks RFA of RMP

NOTE: Small NA components strongly affect the stability and transport.

3D MHD Equilibrium

MHD equilibrium

MHD equilibrium is defined by following equations.

$$\mathbf{J} \times \mathbf{B} = \nabla p$$

$$\nabla \times \mathbf{B} = \mathbf{J}$$

$$\nabla \cdot \mathbf{B} = 0$$

If we can assume the symmetry along the toroidal direction, MHD equilibrium equations are reduced to one equation, so-called the Grad-Shafranov equation.

$$R\frac{\partial}{\partial R}\left(\frac{1}{R}\frac{\partial \Psi}{\partial R}\right) + \frac{\partial^2 \Psi}{\partial Z^2} = -\mu_0 R^2 \frac{dp}{d\Psi} - \frac{1}{2}\frac{dF^2}{d\Psi}$$

The G-S equation is an elliptic partial differential equation.

This means the MHD equilibrium calculation is the boundary value problem.

3D MHD equilibrium

In the 3D system, there are no unique equation like the G-S equation!

In limited cases, we can derive a similar equation to the G-S equation.
=> Stellarator expansion or averaged method.
=> Possible for only conventional stellarator and heliotron for large A_p.

Question:

How to resolve MHD equilibrium equations in 3D?

1. Direct calculation by the iterative method => **PIES**, KITES
2. Energy principle => BETA,**VMEC**, NSTAB
3. Initial value problem by DNS => **HINT/HINT2**

Variational Principle

If we can define the total energy as the functional,

$$W = \int \left(\frac{|B|^2}{2\mu_0} + \frac{p}{\Gamma - 1} \right) dV$$

The first variation means the MHD equilibrium

$$\delta W = 0$$

=> Variational Principle by Grad, Shafranov, Kruskal-Kulsard

Garbedian et al., developed the BETA code based on the variational principle.

Some codes were developed in following the BETA code.

Chodura-Shuelter, NEAR, **VMEC**, BETAS, NSTAB, SIESTA

Remarks of inverse representation

The BETA (or VMEC) code used the inverse representation with an assumption of existence of nested flux surfaces.

The VMEC code is another code based on the variational principle.
Spectral method and improved inverse representation are used.

$$\boldsymbol{B}_i(R,\phi,Z) \Rightarrow \boldsymbol{X}_i(\rho,\theta,\phi)$$

Assuming nested flux surfaces

Existence of nested flux surfaces is a constraint in the variation!

The BETA (VMEC) calculates the "weak solution" (approximated solution)!

Difficulties in 3D MHD equilibrium

Singularity of parallel current

$$\frac{\mathbf{J}\cdot\mathbf{B}}{B^2} = p' \sum \frac{mB_{mn}(s)}{n - \iota m} \cos[m\theta - (n - \iota m)\phi]$$

Singularity appears on rational surface.

Magnetic islands might be opened on every rational surfaces.

If magnetic islands are sufficiently small, assumption of nested flux surfaces can be worked.

Different idea: stepped pressure profile (R. Dewer, et al.)

Difficulties in 3D MHD equilibrium (cont'd)

Magnetic island and stochastization in 3D MHD equilibrium

In 3D MHD equilibrium calculations, magnetic islands and stochastic field naturally appear.

Question:

Why do magnetic islands and stochastic field appear?
Physical? and Numerical?

Answer:

Yes! Physical! Reiman and Boozer predict theoretically nonlinear couplings of resonant and non-resonant components make magnetic islands and stochastic field. (Global effects)
This is different physics to the layer theory. (Local effects)

Global effects or Local effects?

$$p \propto 7-11s+4s^2$$

vacuum β~2% β~3%

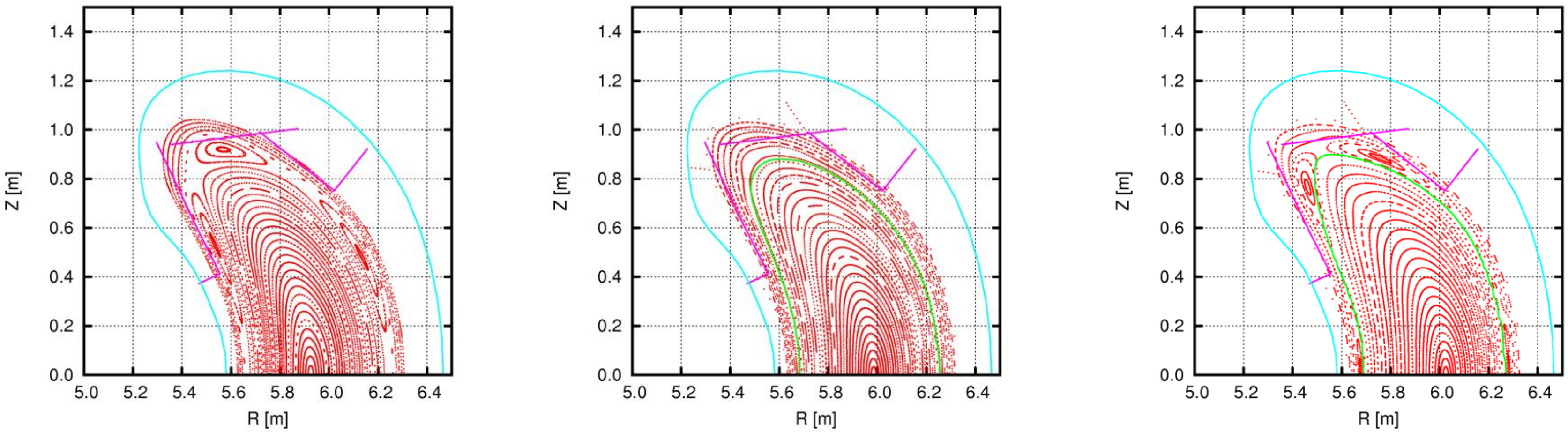

- Clear flux surfaces are kept with increasing β.
- 5/6 islands shrink due to increasing β.
- For β~2%, islands are almost healed.
- For β>3%, the phase of 5/6 islands changes.

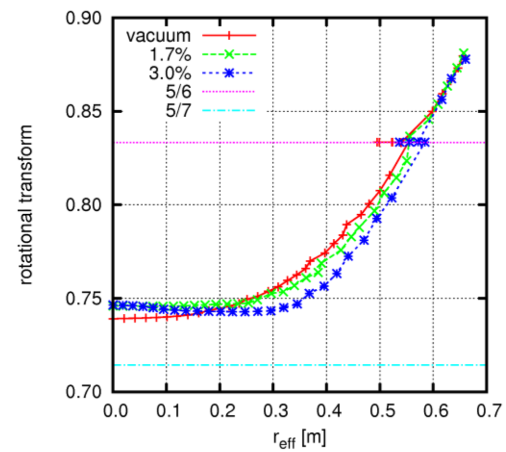

Islands are healed without resonant current on 5/6 rational surface.

→ Contributions of non-resonant components.

Control Coil Variation Changes Flux Surface Topology

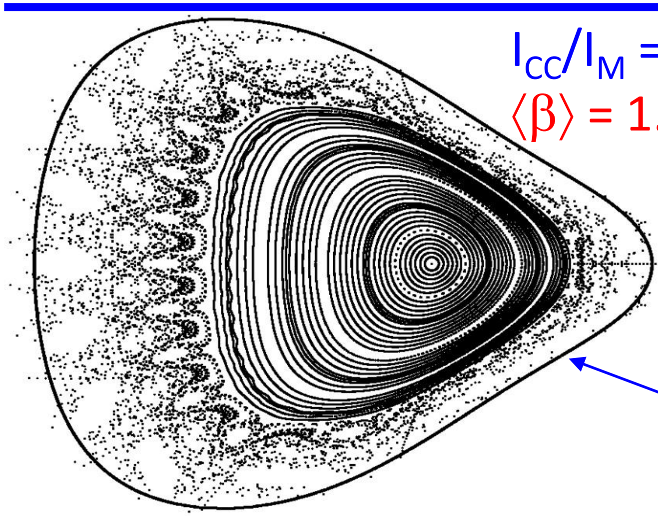

$I_{CC}/I_M = 0$
$\langle\beta\rangle = 1.8\%$

VMEC boundary

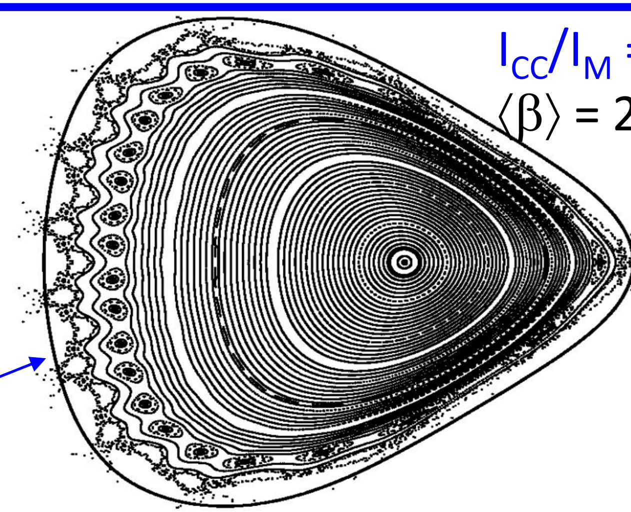

$I_{CC}/I_M = 0.15$
$\langle\beta\rangle = 2.0\%$

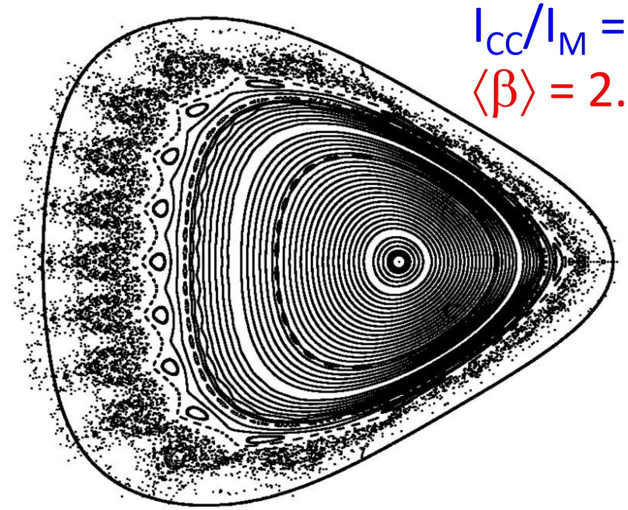

$I_{CC}/I_M = 0.15$
$\langle\beta\rangle = 2.7\%$

- PIES equilibrium analysis using fixed pressure profile from equilibrium fit (not yet including current profile).
- Calculation: at ~ fixed β, I_{CC}/I_M=0.15 gives better flux surfaces
- At experimental maximum b values
  -- 1.8% for I_{CC}/I_M =0
  -- 2.7% for I_{CC}/I_M = 0.15
  calculate similar flux surface degradation

Courtesy to M.C.Zarnstorff and A.H. Reiman

Edge T_e does not respond to P_{inj}

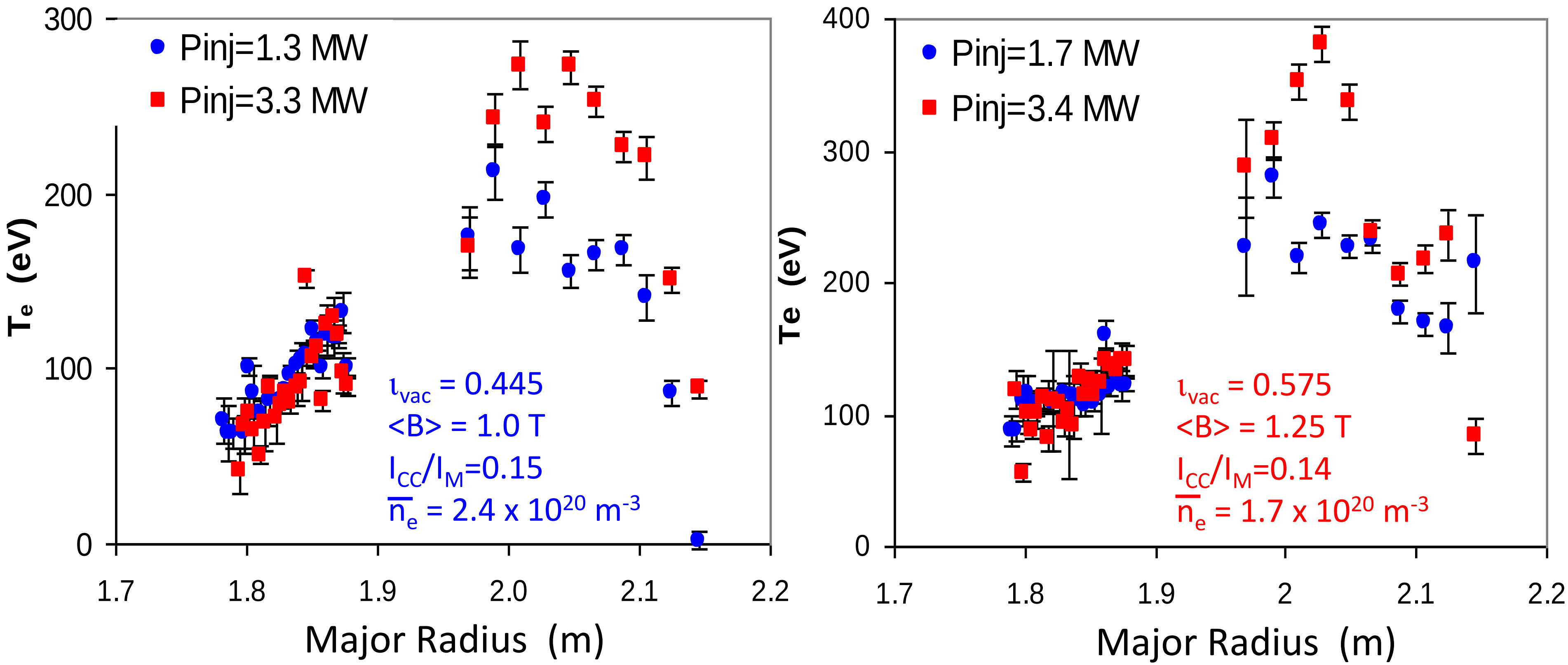

- Edge T_e and ∇T_e does not change with increasing P_{inj} !!
  $\Rightarrow$ Radial transport degrading as power increases
- Fixed density, and constant n_e profile. Increase in β due to core T_e increase
- Edge ∇T_e lower for $\iota = 0.575$ $\Rightarrow$ higher radial transport.

Courtesy to M.C.Zarnstorff and A.H. Reiman

3D MHD Equilibrium studies

1. Equilibrium Beta Limit in heliotron

High-beta Steady State Discharge

- $\langle\beta\rangle_{max}$ ~ 4.8 %, β_0 ~ 9.6 %, H_{ISS95} ~ 1.1
- Plasma was maintained for $85\tau_E$
- Shafranov shift Δ/a_{eff} ~ 0.25
- Peripheral MHD modes are dominantly observed.

R_{ax} = 3.6 m, B_t = -0.425 T

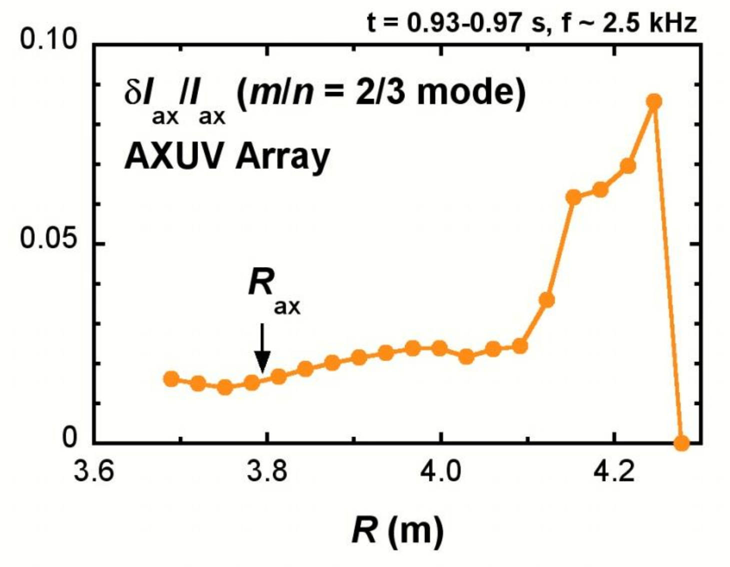

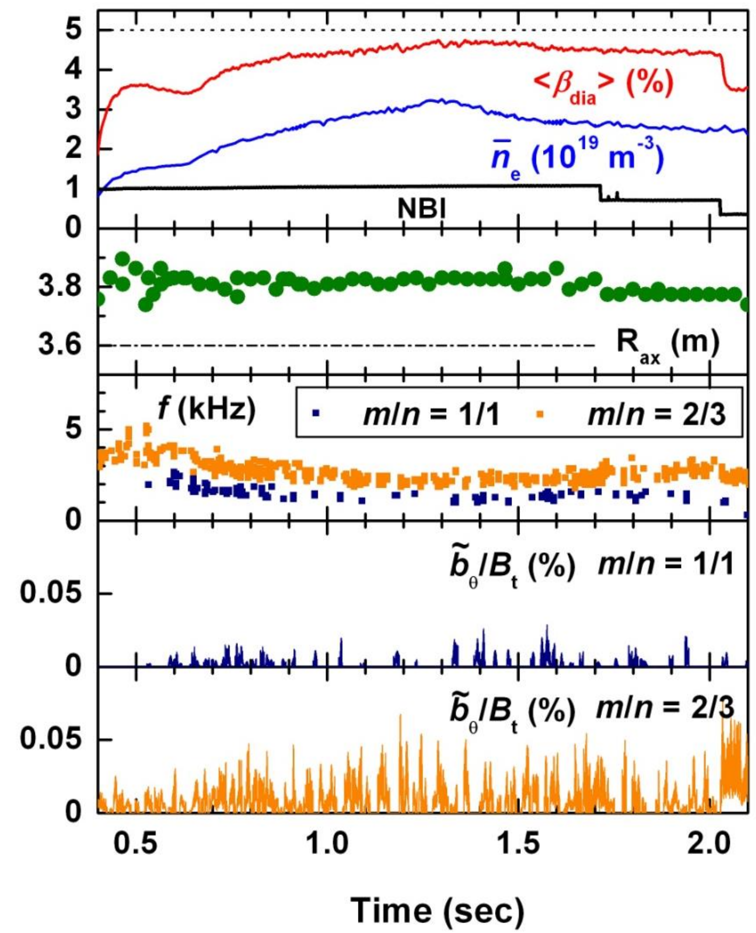

High-beta Discharge – Pellet Injection –

- Perpendicular-NBI was applied after several pellets were injected and tangential NBI is turned off which leads to reduction of Shafranov shift.

- MHD activity is not enhanced in high-beta regime with more than 4 %

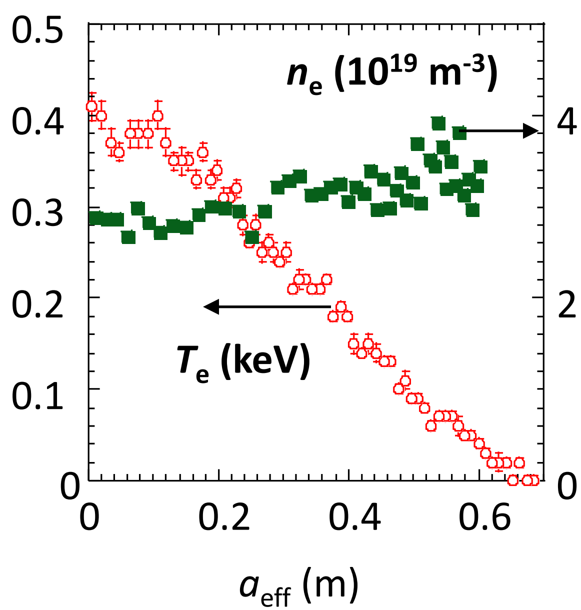

R_{ax} = 3.6 m, B_t = -0.425 T

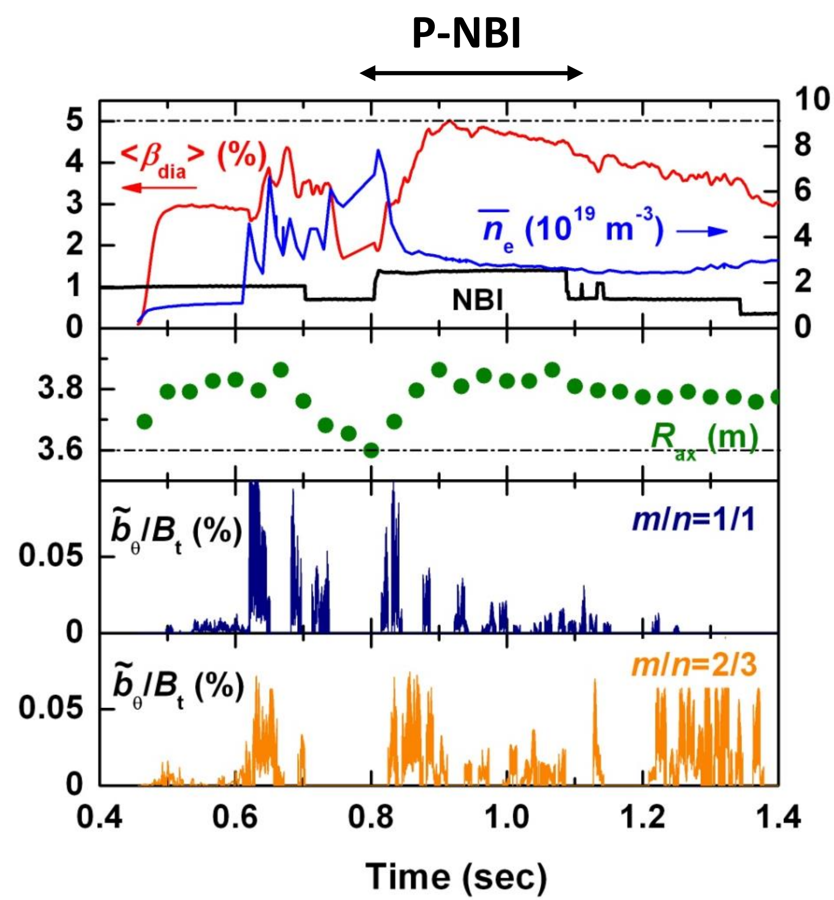

How about is the magnetic surface topology?

Degradation of flux surfaces due to increasing β

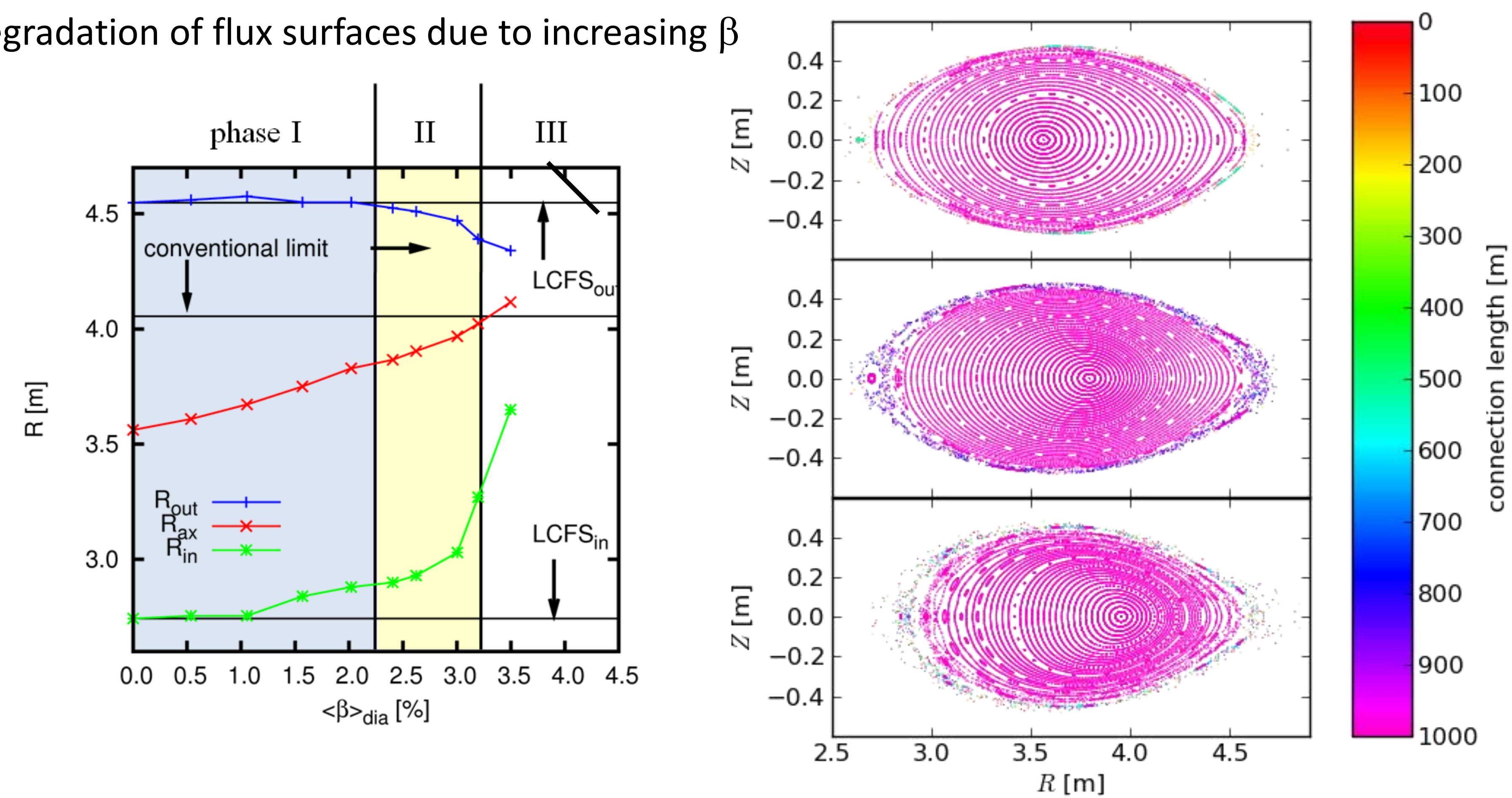

In the peripheral region, magnetic field lines become stochastic as b increases.
The volume inside LCFS shrinks drastically.

Results of HINT2 analyses

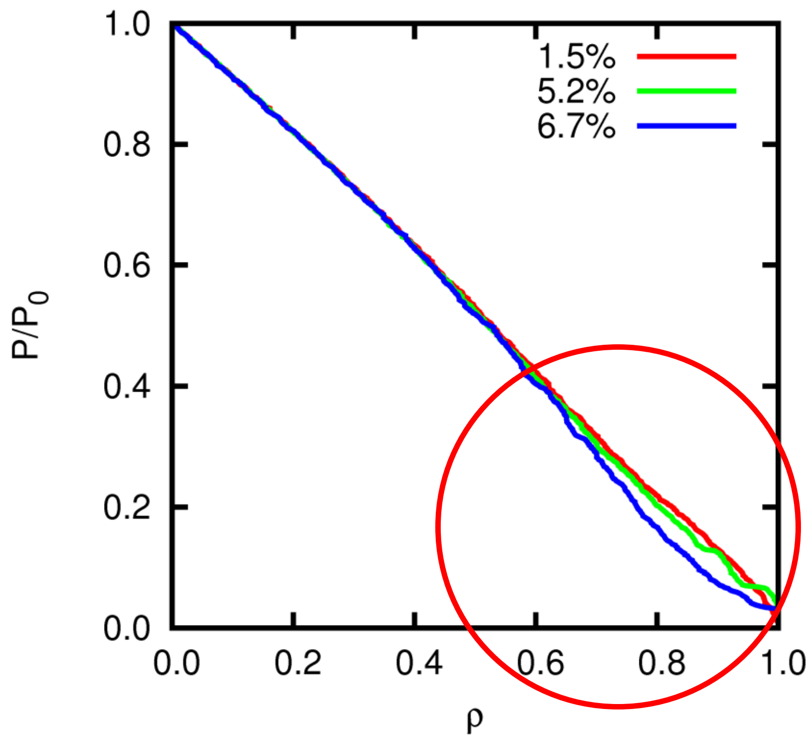

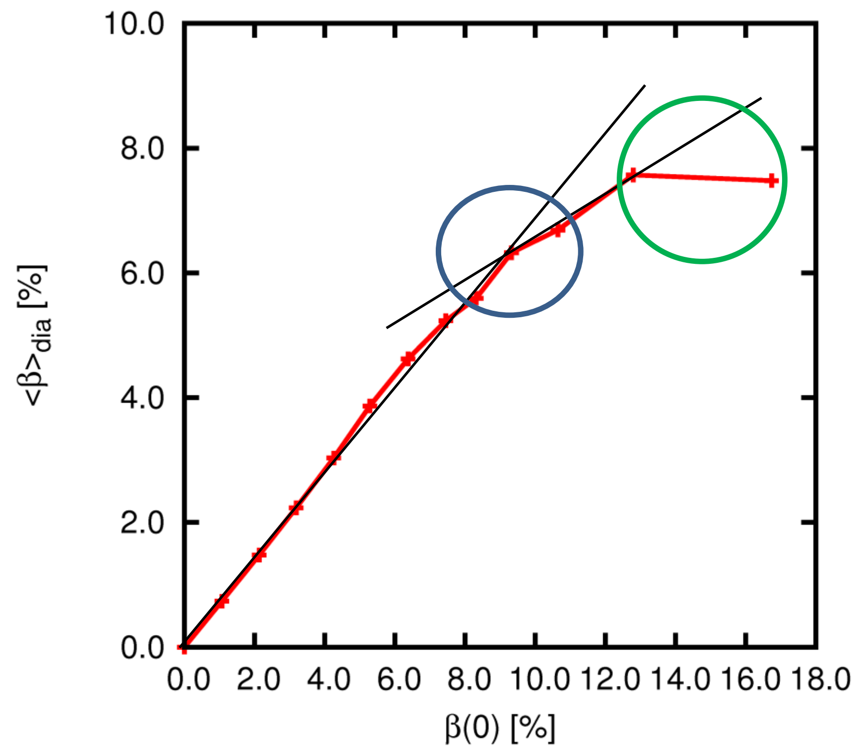

For β>6.7%, the fixed pressure profile is reduced at ρ>0.6.

The slope of <β> changes due to the reduction of the pressure profile.

The change of the slope is a good index of the equilibrium beta limit.
Note: this index is a soft limit of the MHD equilibrium.

Results of HINT2 analyses: Beyond the index

Proposed index is the soft limit. That is, the beta can be still increased.

What is most critical limit?

With large Shafranov shift, the separatrix appears near the axis.

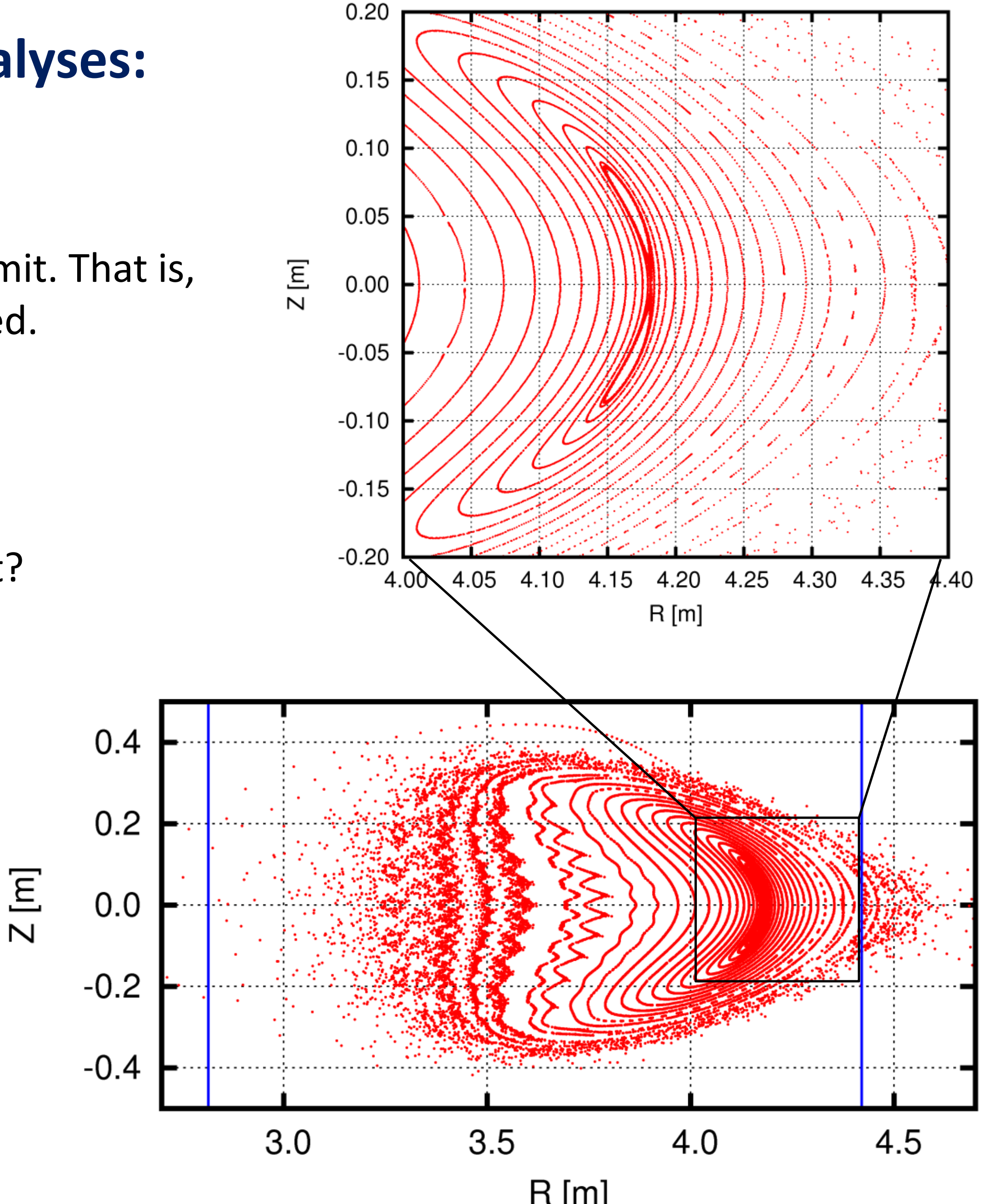

Results from HINT well describes deformation of magnetic surfaces

3-D equilibrium consistent with experimental observation, i.e., Shafranov shift, pressure profile, etc.

Significant pressure (T_e) gradient exists in the edge stochastic area

Hypothesis

1) Plasma heals flux surfaces
2) Profile is consistent with characteristics of stochastic field
3) Somewhere between 1) & 2)

$L_{C\text{-}TB}$: connection length between the torus-top and - bottom

✓ L_C >> $L_{C\text{-}TB}$

➔ Pfirsch-Schlüter current is effective

➔ Secure MHD equilibrium

✓ L_C >> MFP (even under a reactor condition)

➔ Plasma is collisional enough to secure isotropic pressure

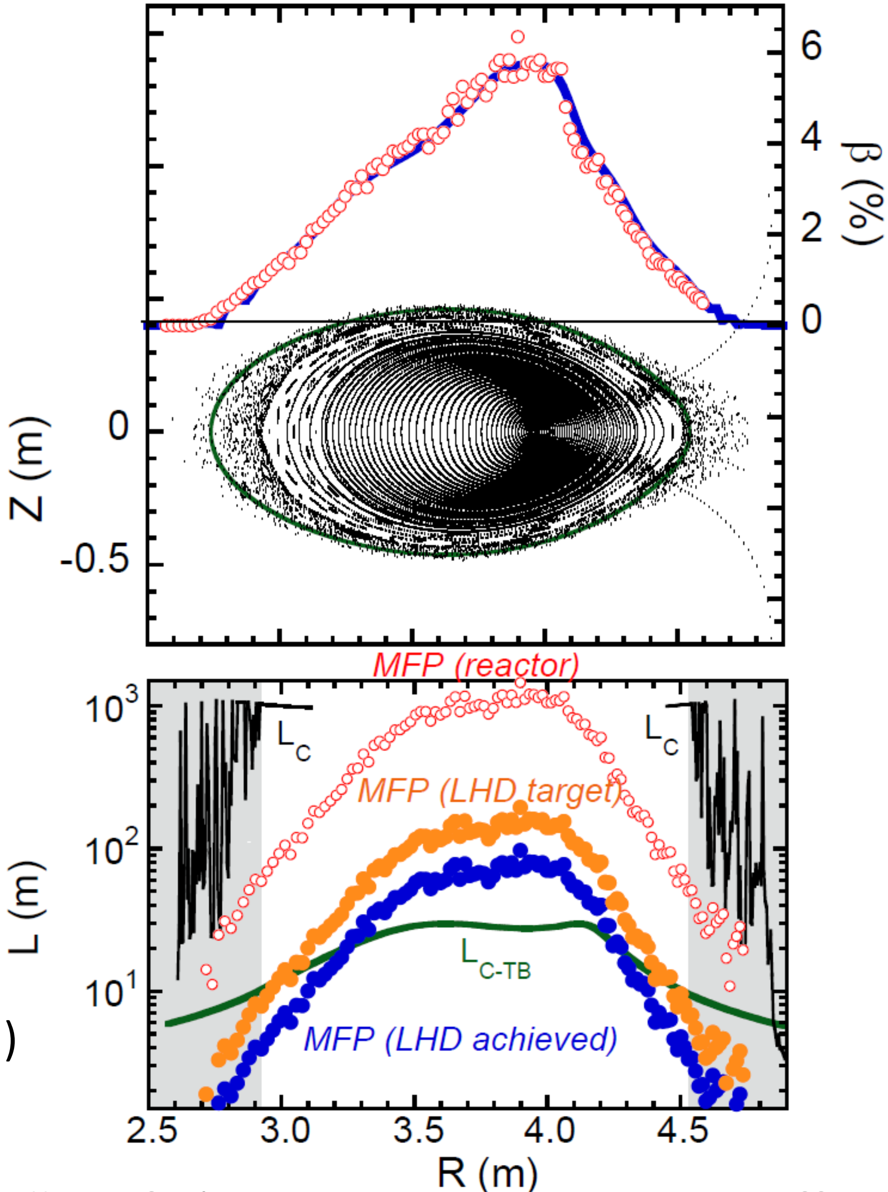

3D MHD Equilibrium studies

2. Experimental studies of 3D MHD equilibrium in LHD

Identification of "last closed" flux surfaces (LCFS)

Free boundary VMEC code is well known theoretical identification method of shape of LCFS. There nested flux surfaces is assumed a-priori even in LCFS.

HINT code has another identification method of shape of LCFS.

According to HINT calculation, at well defined LCFS, a finite pressure exists.

Check the validity of identification method of shape of LCFS through the observed shift of mag. surf.

LHD, R_{ax}=3.6m conf.
$<\beta_{dia}>$~2.7%

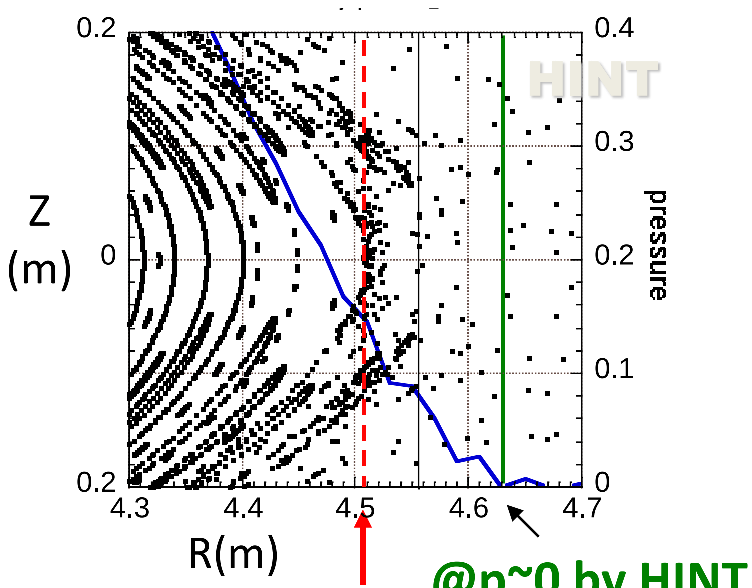

Free boundary VMEC: developed by S.P.Hirshman, P.merkel et al.
HINT: no assumption of flux surfaces, developed by T.Hayashi et al. In right figure, p=0 is set when the field line connect a wall before it toroidally turns 5 times.

Shift of flux surface and magnetic axis

An equilibrium data is selected so as to fit T_e profile measured by Thomson scattering measurements the best among an equilibrium database with various beta values and their profiles.

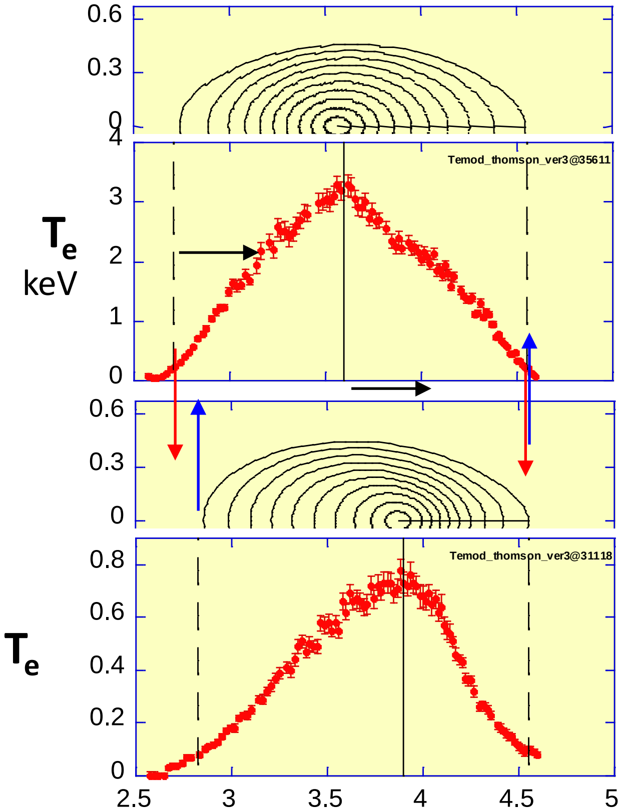

=>

Center of Last Closed Flux Surface (LCFS) and magnetic axis are estimated from the best fitting equilibrium data.

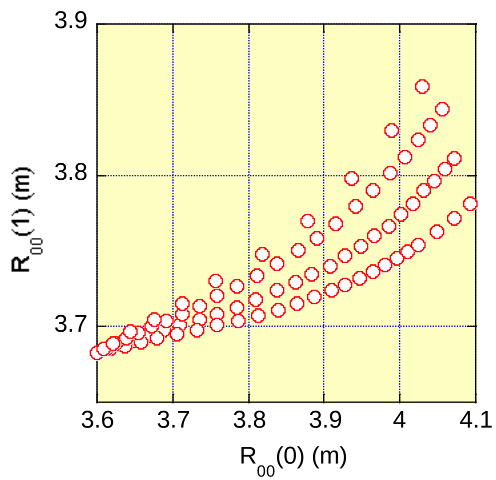

Assumed pressure profiles
[β~$(1-\rho^2)^2$, $(1-\rho^2)(1-\rho^8)$, $(1-\rho^4)(1-\rho^8)$, $(1-\rho^8)^2$]

Diagram of geometrical center and magnetic axis in the equilibrium database.

Shift of flux surface and magnetic axis

Experimental results vs. prediction by HINT

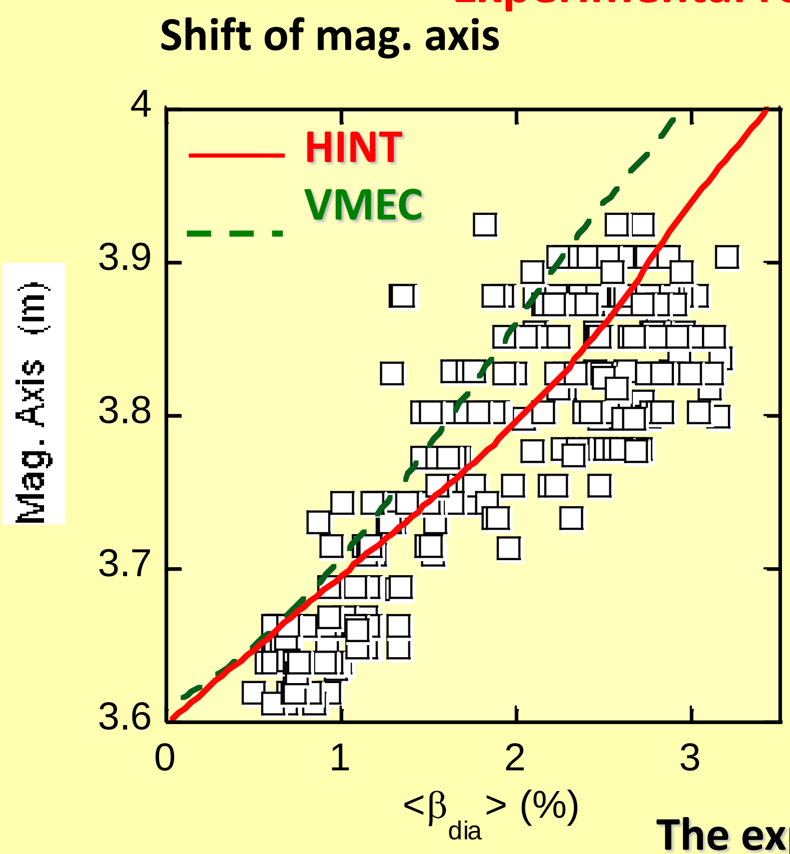

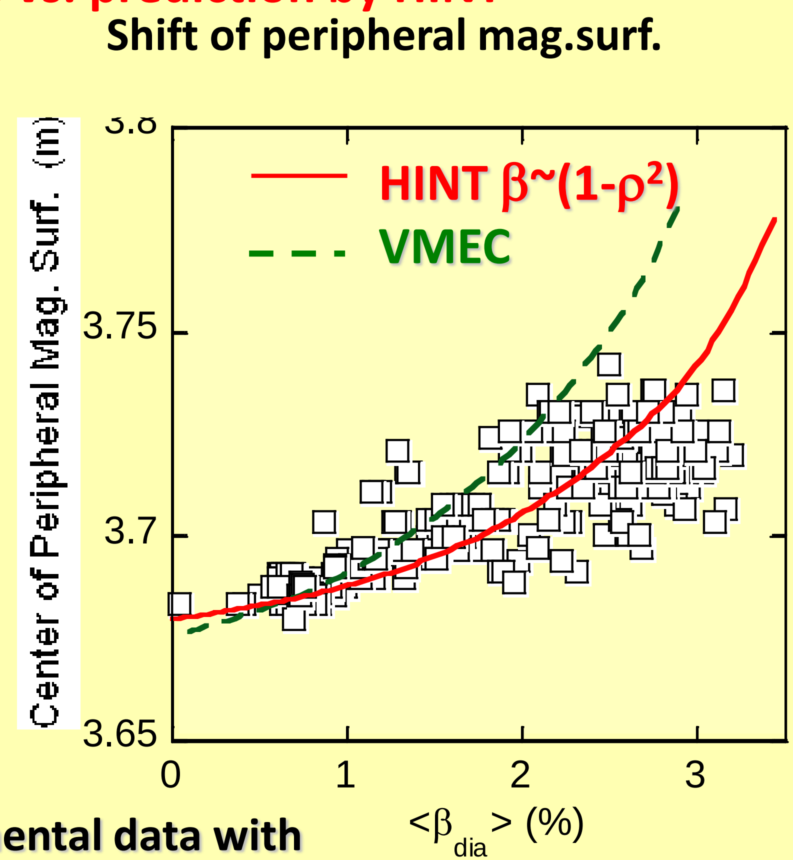

The experimental data with $\beta \sim (1-\rho^2)$ are extracted.

Beta dependences of observed shift of mag.axis and peripheral mag. surf. are consistent with the prediction by HINT code.

Comparison between observed pressure and prediction

Well defined LCFS in vacuum.

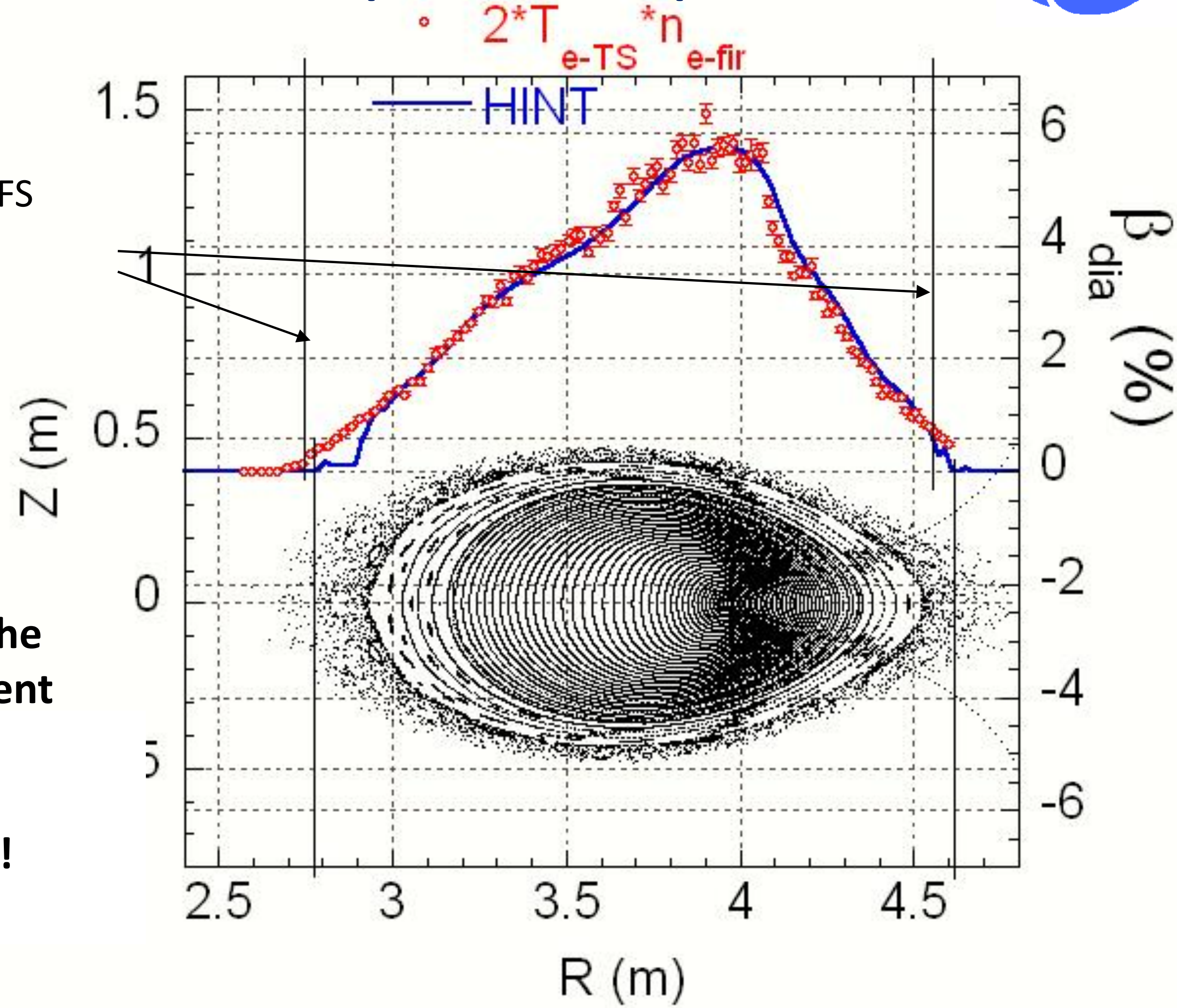

Plasma exists over the predicted confinement region due to HINT code
=> due to diffusion?!

Beta dependence of effective plasma "volume"

Here "effective plasma volume" is defined as the volume has an amount (99%) of electron thermal energy

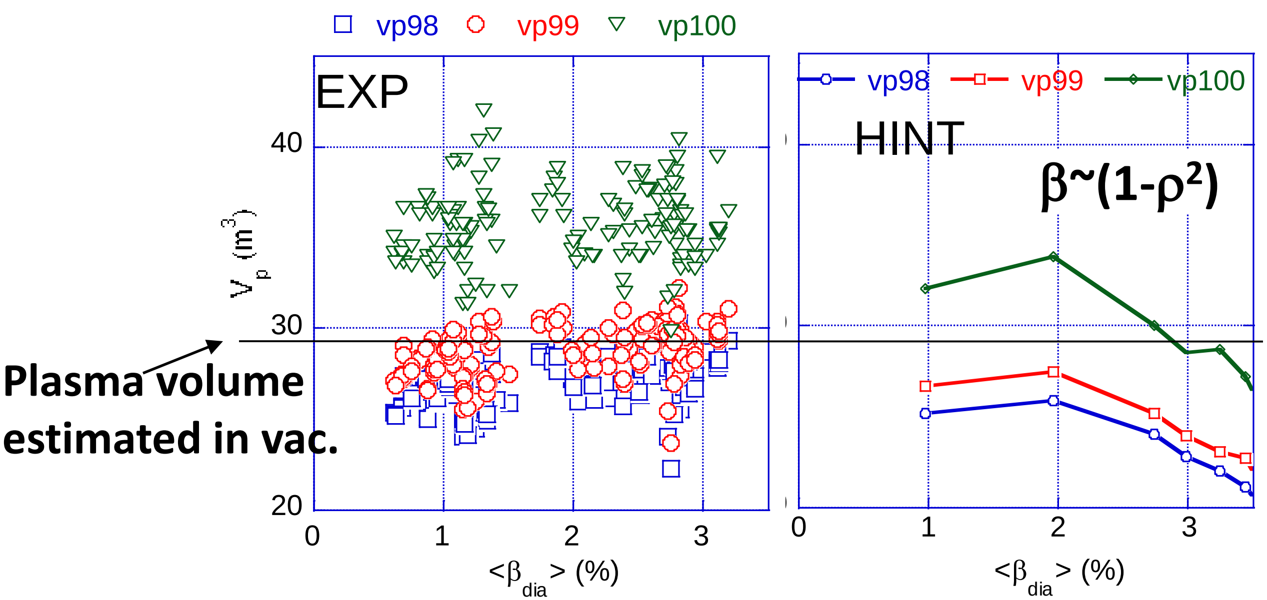

vp98,99,100
=>
the volume with 98%, 99% and 100% of the total electron pressure

As systematic observation, plasma exists over the predicted confinement region due to HINT code
=> due to diffusion?!
Beta dependence of the effective plasma volume is not clear.

Beta dependence of effective plasma "boundary"

The experimental data with β~(1-r²) are extracted.

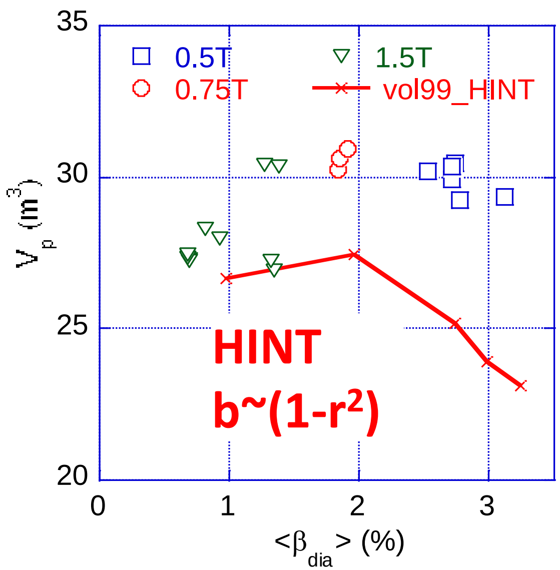

"volume"

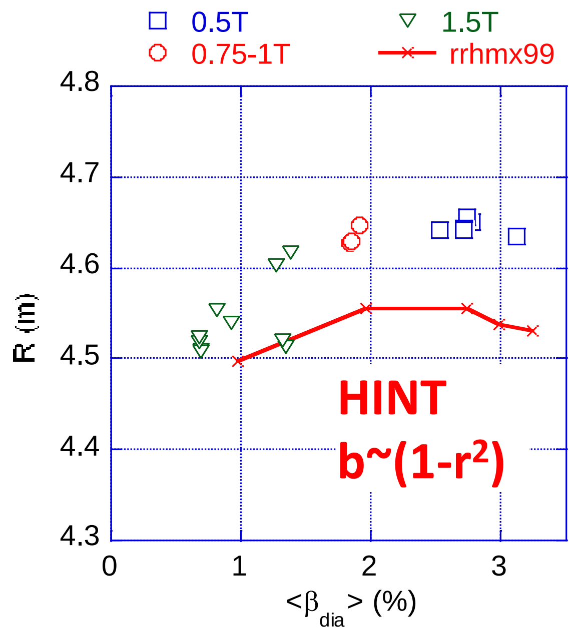

"torus outboard boundary"

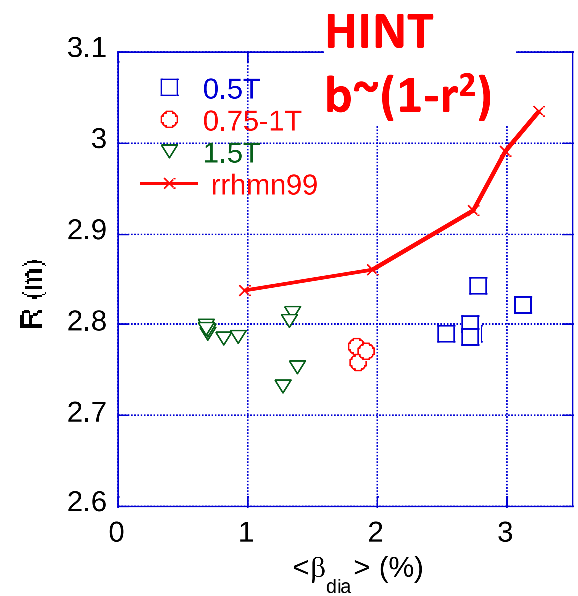

"torus inboard boundary"

The decrease of plasma "volume" has not observed up to β~3%, which corresponds to no shift of "torus inboard boundary" in high beta range.

What identification method of the effective plasma boundary is the most valid ?

Comparisons between Er measurement and numerical modeling

3D MHD equilibrium analyses suggest :

1. Magnetic filed lines become stochastic by the "***3D plasma response***".
2. But L_C is still long in the stochastic region.
   -> Stochastic region is still the confinement region.
   -> "***effective plasma boundary***" is not the LCFS.

Comparison with HINT2 modeling

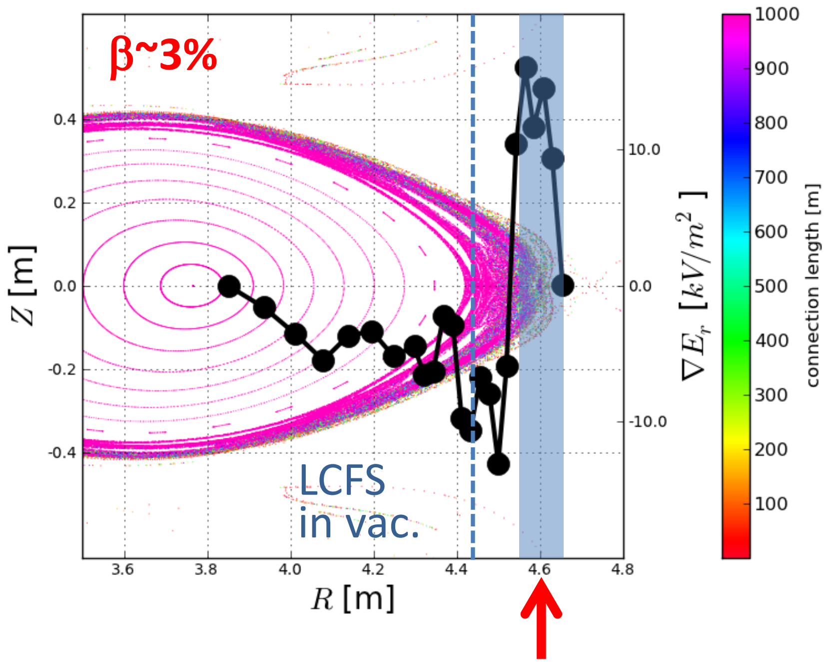

max E_r shear appears in stochastic region

Contours of connection length with different β

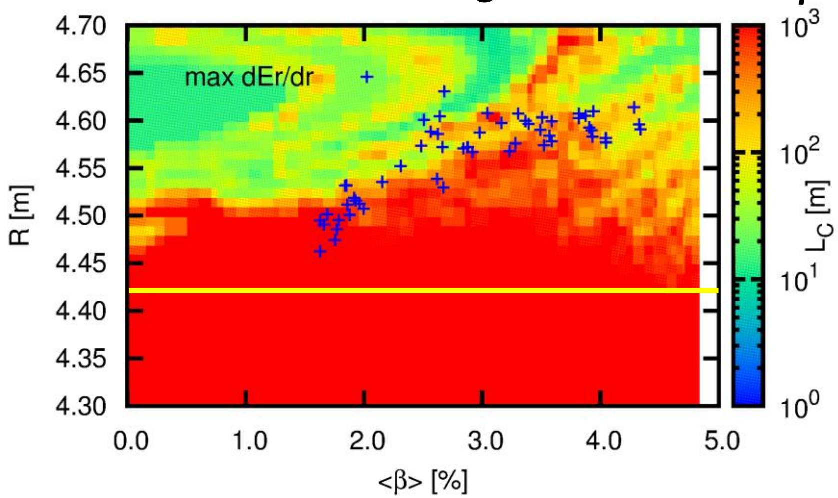

- L_C is long in the outward of the torus.
- Short L_C appears due to increased β.
- Positions of max E_r shear correlate contours of L_C.
- Position of max E_r shear appears in short L_C.

Is the position of max E_r shear decided by L_C?

Change of heat plus propagation by RMP

Joint experiment with DIII-D group proposed by Dr. T. Evans.

Magnetic tpology

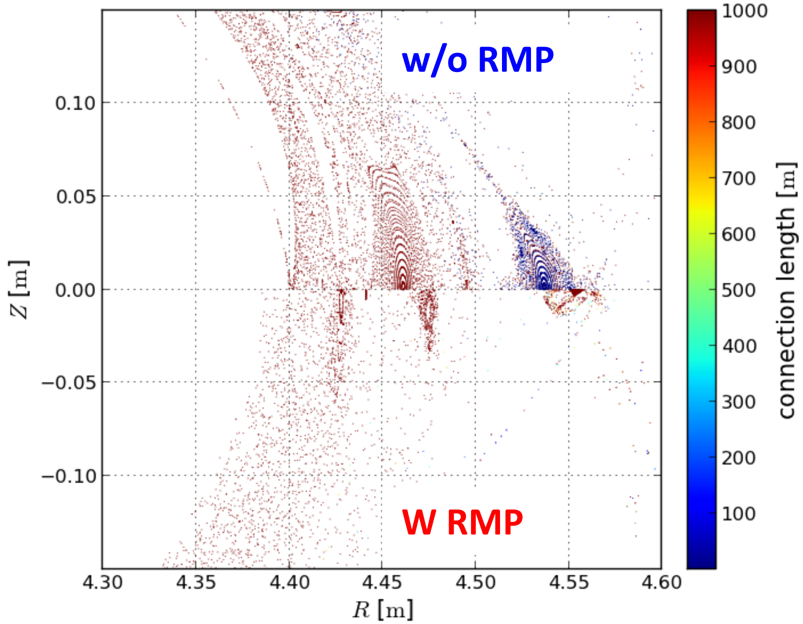

Er

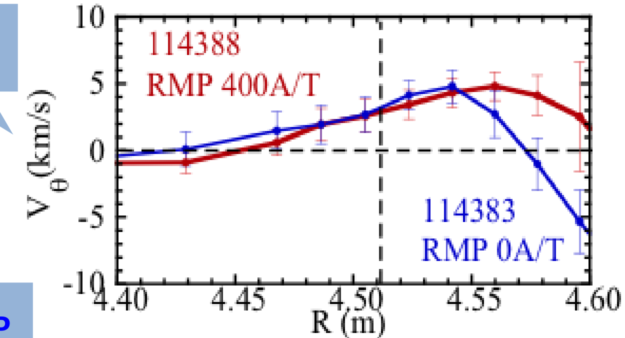

w/o RMP

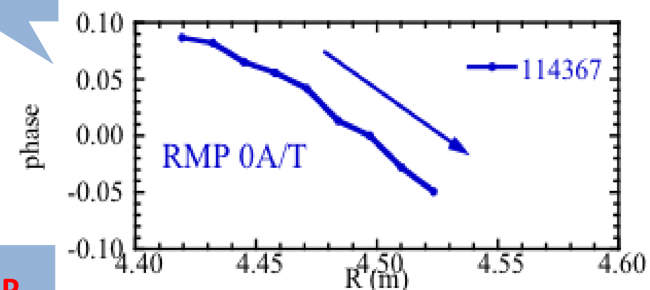

W RMP

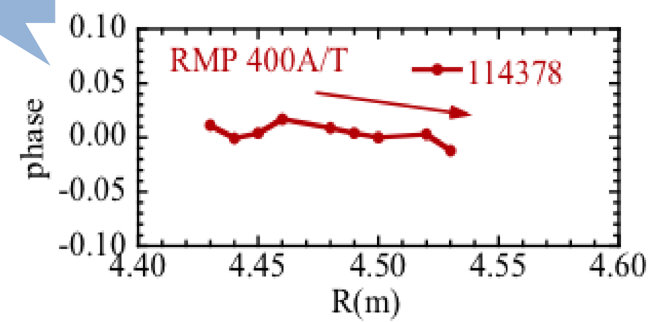

We observed difference of heat plus propagation w or w/o RMP.

=> We will apply to DIII-D experiment.

3D MHD Equilibrium studies

3. Identification of 3D plasma boundary by CCS

Cauchy Condition Surface (CCS) Method

to identify plasma boundary shape from signals of magnetic sensors located outside the plasma

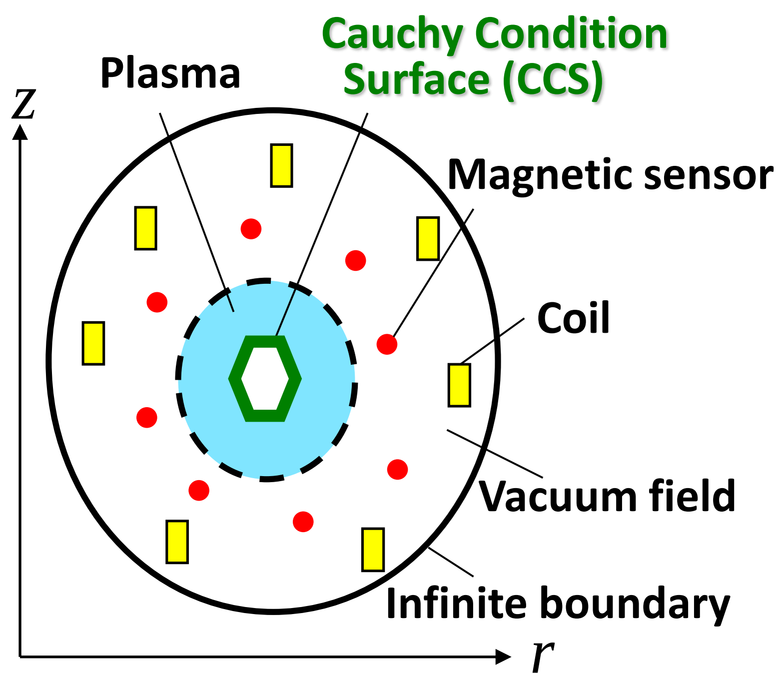

Solve boundary integral equations, Assume vacuum field outside CCS.

(The effect of plasma current is transformed into the CCS.)

2-D CCS analysis

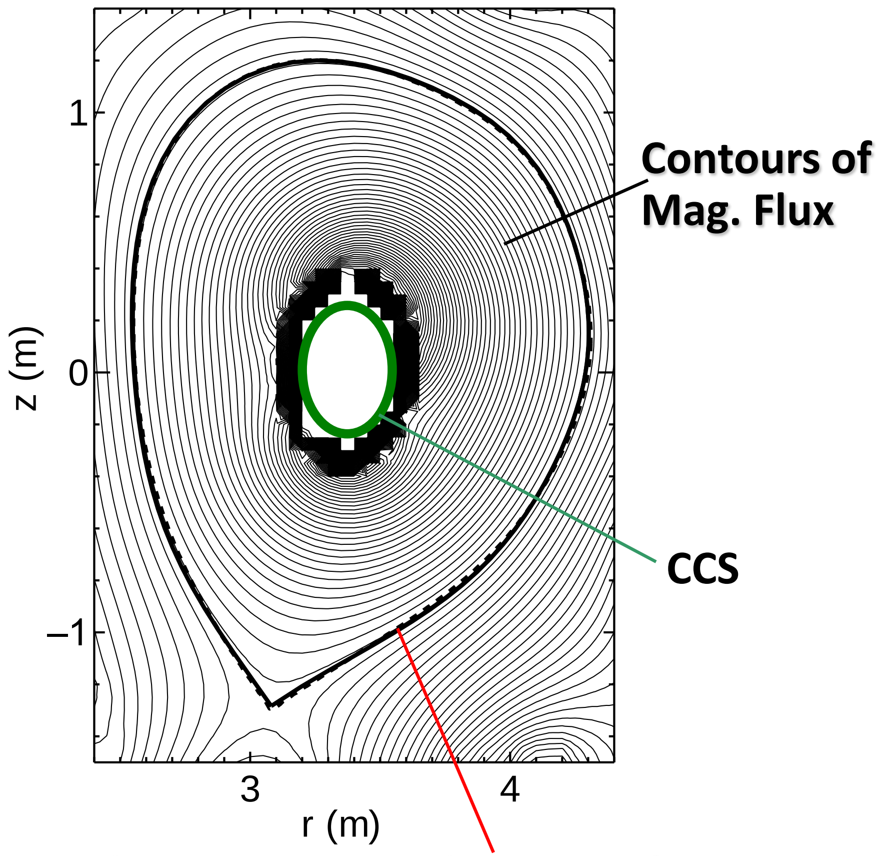

The outermost closed surface =Plasma Boundary

Difference between 2-D and 3-D CCS method

	2-D CCS	*3-D CCS*
Governing equation	Grad-Shafranov equation	3-D Laplace equation
No. of boundary elements	3	48 （Rotational symmetry considered）
No. of unknowns	12	2592 （Rotational symmetry considered）
Condition number	$\sim 10^{6}$	$>10^{15}$ （$\sim 10^{5}$）
Unknowns on the CCS	$\psi, \dfrac{\partial \psi}{\partial n}$ （scalar）	$A, \dfrac{\partial A}{\partial n}$ （vector）
How to calculate B	$B_r = -\dfrac{1}{r}\dfrac{\partial \psi}{\partial z}, \quad B_z = \dfrac{1}{r}\dfrac{\partial \psi}{\partial r}$	$\boldsymbol{B} = \nabla \times \boldsymbol{A}$
Mag. Surface function ψ	$\psi = rA_{\varphi} \; (\mathbf{B} \cdot \nabla \psi = 0)$	ψ = ?
How to identify the boundary	*Flux contour* 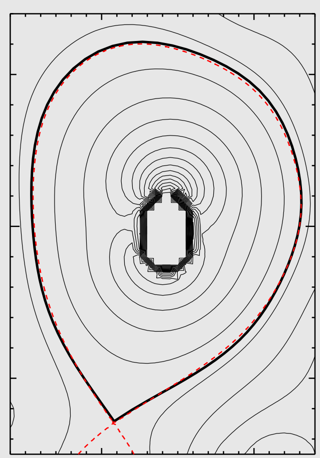	*Mag. Field line tracing* 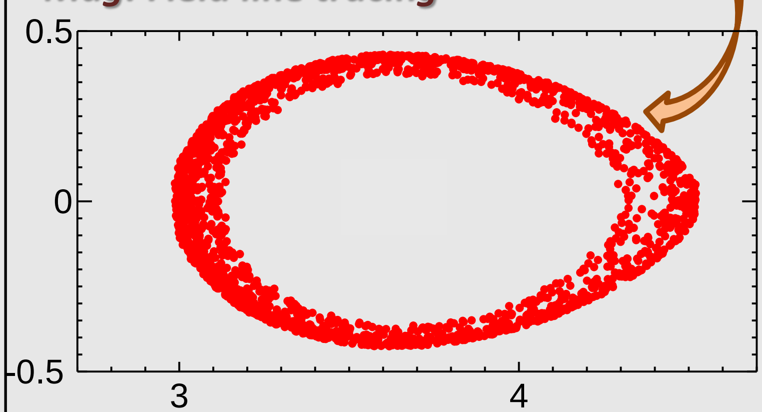

Why 3-D CCS method is challenging?

- Huge number of unknowns
  => Need large no. of sensors
  => the problem becomes ill-conditioned
- No mathematical expression of magnetic surface function ψ for a helical device
  (*cf.* $\psi = r\,A_\varphi$ for a tokamak)

Large Helical Device (LHD)

- The plasma current is much weaker than the current in a tokamak device.
- Dominant is the Pfirsch-Schülter current, the average of which over a mag. surface is zero, but still has a 3-D profile.

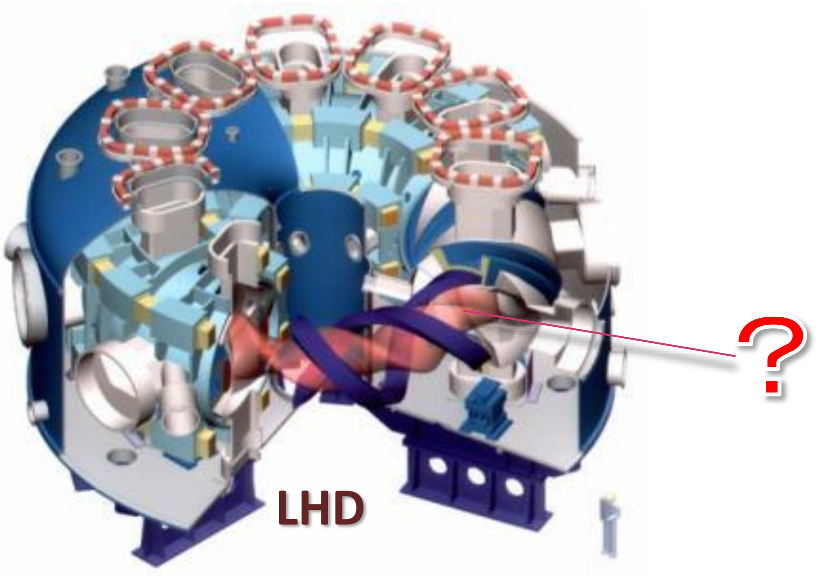

Calculation Model for the LHD

Mag. sensors arranged a little way outside the plasma

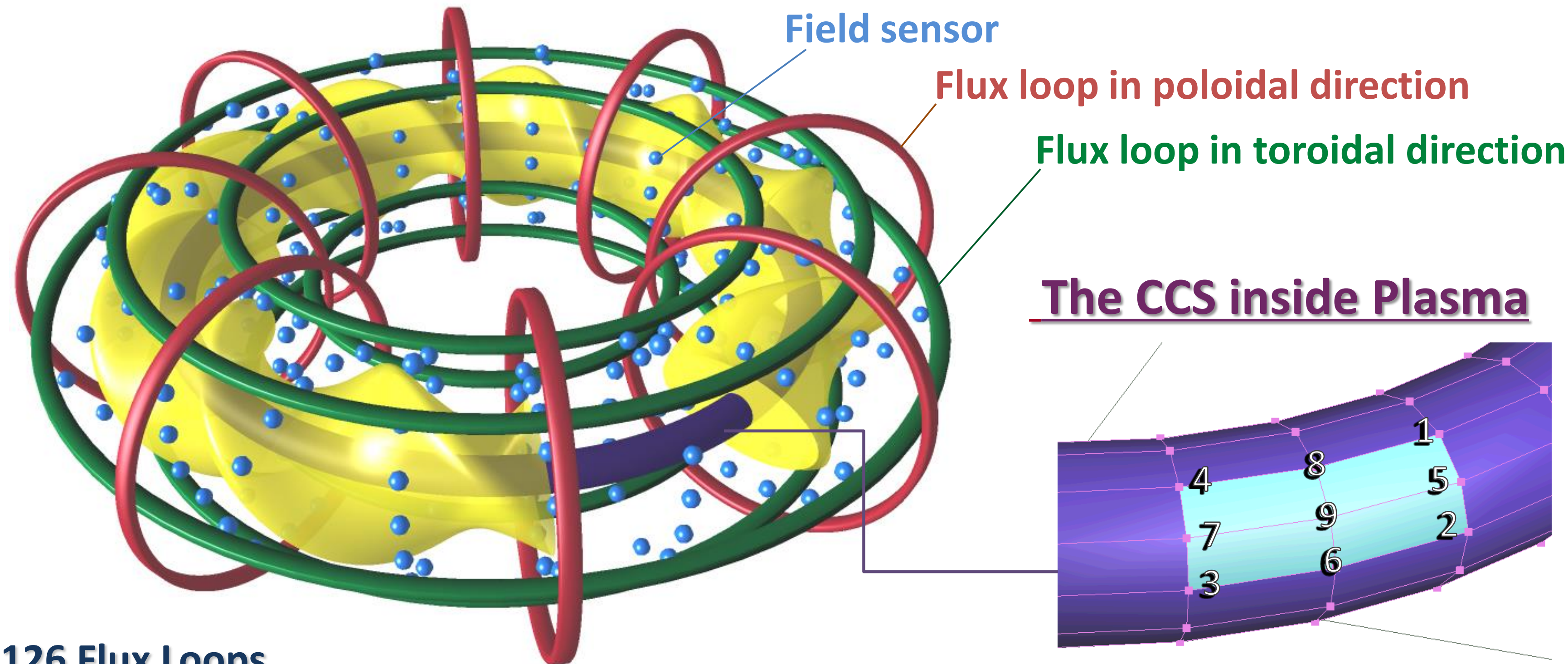

126 Flux Loops
(100 toroidal; 26 poloidal)
440 Field Sensors

Consider 10-fold rotational symmetry,
Only 36-deg. portion of CCS was modeled.

Signal values were calculated beforehand using the HIN2 code.

Divided into 48 boundary elements (each has 9 nodal points)

Last closed magnetic surface (LCMS):

the outermost closed surface that is recognized through field line tracing.

Region	Definition	Current density	Accuracy of the reconstructed field
Vacuum	Outside the stochastic region	No	Valid
Stochastic	The field lines reach the divertor plate	Weak	Fair
"Dirty"	Sandwiched between LCMS & CCS	Strong	Large error
"Black"	Inside the CCS	Strong	Out of the analysis

Distribution of absolute error B_φ

$$\varepsilon = \left| B_{\mathrm{CCS}} - B_{\mathrm{Ref}} \right| \ \ (\mathrm{T})$$

(*The reference solution B_{Ref} were provided using the HINT2 code.*)

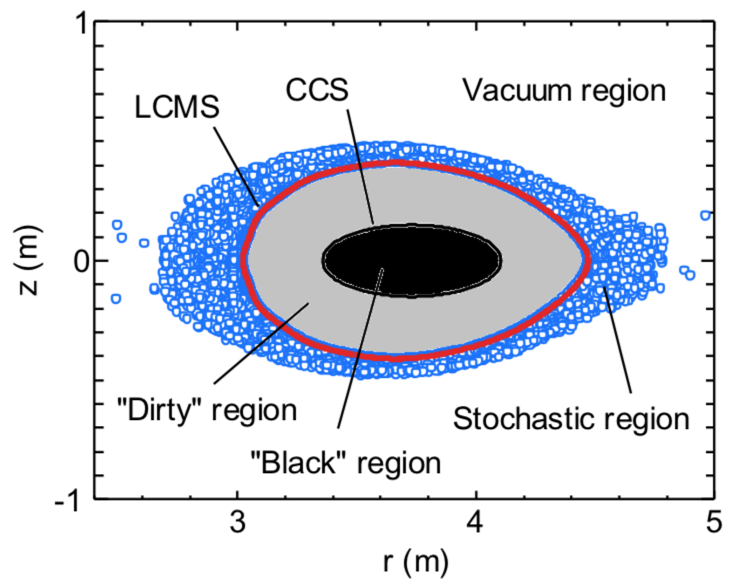

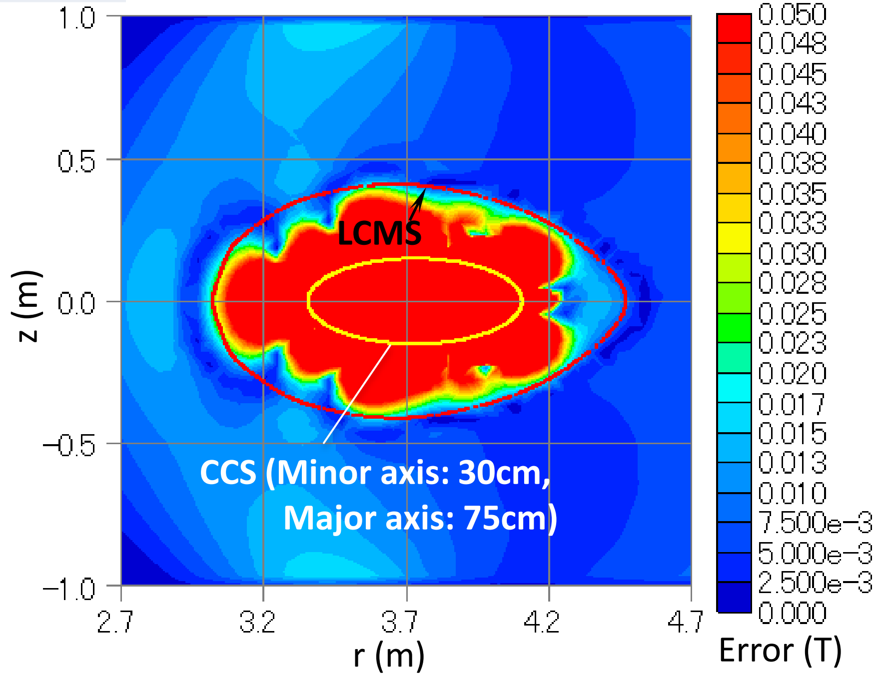

Variation in 'Inside/Outside' Ratio

$$R_{I/O} = s_{inside}^2 / s_{outside}^2$$

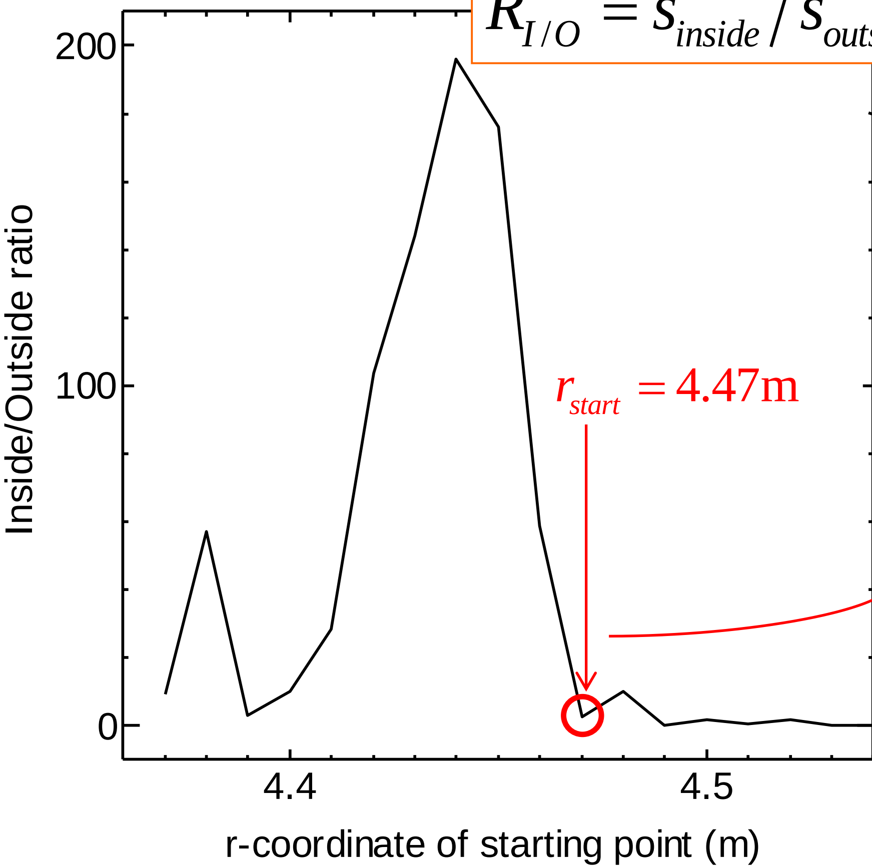

The **scatter** is given by $s^2 = \dfrac{1}{m}\sum_{j=1}^{m} d_j^{\,2}$,

where $d_j^{\,2}$ denotes the distance between the reconstructed magnetic surface and the *j*-th point in the *m* Poincaré plot points.

Extracted from contours of quasi magnetic surfaces

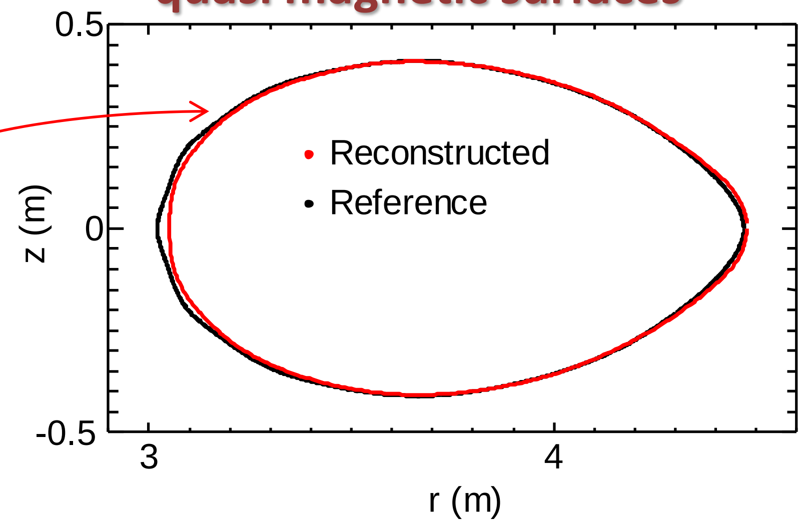

The ratio jumps at $r_{start} = 4.47\mathrm{m}$, which corresponds to **the LCMS**, **the entrance to the 'dirty region'.**

This extracted LCMS agrees well with the reference LCMS.

Conclusion

1. 3D MHD equilibrium studies are discussed.
2. In the LHD configuration, 3D MHD equilibrium calculation predicts the stochastization due to increase β. This leads the beta limit.
3. 3D MHD equilibrium calculations are compared systematically with experimental observations. HINT results are more reliable than VMEC results. To study further, the identification of the plasma boundary and topology is very important.
4. Identification of 3D plasma boundary by CCS is discussed.

Extension of 3D MHD equilibrium

- All 3D MHD equilibrium calculation code can calculate only magnetic-static equilibrium.
- Almost codes assume the isotropic plasma pressure.

Studies of anisotropic plasma pressure and rotation are critical and urgent issues!